

Magnetic properties of a spin-orbit entangled $J_{\text{eff}} = 1/2$ three-dimensional frustrated rare-earth hyperkagome

B. Sana,¹ M. Barik,¹ M. Pregelj,^{2,3} U. Jena,¹ M. Baenitz,⁴ J. Sichelschmidt,⁴ K. Sethupathi,^{1,5} and P. Khuntia^{1,5,*}

¹*Department of Physics, Indian Institute of Technology Madras, Chennai, 600036, India*

²*Jožef Stefan Institute, Jamova cesta 39, 1000 Ljubljana, Slovenia*

³*Faculty of Mathematics and Physics, University of Ljubljana, Jadranska u. 19, 1000 Ljubljana, Slovenia*

⁴*Max Planck Institute for Chemical Physics of Solids, Nöthnitzer Strasse 40, 01187 Dresden, Germany*

⁵*Quantum Centre of Excellence for Diamond and Emergent Materials, Indian Institute of Technology Madras, Chennai, 600036, India*

The interplay between competing degrees of freedom can stabilize non-trivial magnetic states in correlated electron materials. Frustration induced strong quantum fluctuations can evade long-range magnetic ordering leading to exotic quantum states such as spin liquids in two-dimensional spin-lattices such as triangular and kagome structures. However, the experimental realization of dynamic and correlated quantum states is rare in three-dimensional (3D) frustrated magnets wherein quantum fluctuations are less prominent. Herein, we report the crystal structure, magnetic susceptibility, electron spin resonance and specific heat studies accompanied by crystal electric field calculations on a 3D frustrated magnet $\text{Yb}_3\text{Sc}_2\text{Ga}_3\text{O}_{12}$. In this material, Yb^{3+} ions form a three-dimensional network of corner-sharing triangles known as hyperkagome lattice without any detectable anti-site disorder. Our thermodynamic results reveal a low-energy state with $J_{\text{eff}} = 1/2$ degrees of freedom in the Kramers doublet state. The zero field cooled and field cooled magnetic susceptibility taken in 0.001 T rules out the presence of spin-freezing down to 1.8 K. The Curie-Weiss fit of magnetic susceptibility at low temperature yields a small and negative Curie-Weiss temperature indicating the presence of a weak antiferromagnetic interaction between $J_{\text{eff}} = 1/2$ (Yb^{3+}) moments. The Yb-electron spin resonance displays a broad line of asymmetric shape consistent with the presence of considerable magnetic anisotropy in $\text{Yb}_3\text{Sc}_2\text{Ga}_3\text{O}_{12}$. The crystal electric field calculations suggest that the ground state is well separated from the excited states, which are in good agreement with experimental results. The absence of long-range magnetic ordering inferred from specific heat data indicates a dynamic liquid-like ground state at least down to 130 mK. Furthermore, zero field specific heat shows a broad maximum around 200 mK suggesting the presence of short-range spin correlations in this three-dimensional frustrated antiferromagnet.

I. INTRODUCTION

Geometrically frustrated magnets have drawn significant attention due to their emergent magnetic phenomena arising from competing interactions and quantum fluctuations [1–4]. Two-dimensional (2D) frustrated magnets are prime contenders to host exotic quantum states with fractional quantum numbers following the seminal proposal of quantum spin liquid state on a triangular lattice antiferromagnet by P. W. Anderson [5]. Frustrated magnets with next nearest-neighbor exchange interaction, bond dependent Ising interactions and magnetic anisotropy are ideal candidates in this context [2, 6]. A quantum spin liquid (QSL) is characterized by the absence of long-range magnetic order despite strong exchange interaction between spins, the absence of local order parameter and spins not freezing down to absolute zero. The spins maintain a highly entangled state in the QSL state, which harbors exotic fractional excitations such as spinons and Majorana fermions that are essential ingredients for future quantum information processing [3, 4, 6–9]. Geometrically frustrated triangular, kagome and hyperkagome lattices, wherein frustration induced strong quantum fluctuations are at play, offer a promising platform for the experimental realization of QSL. The identification of associated non-trivial quasi-particles and their interactions

in the QSL state is an attractive track in quantum condensed matter. The exotic excitations in the QSL state are completely different from spin-wave excitations observed in conventional magnets with static order [1, 2, 6]. There are reports on a quite good number of promising two-dimensional quantum spin liquid candidates, however a very few 3D quantum spin liquids are studied so far [7, 8, 10–31].

Remarkably, an excellent three-dimensional lattice to realize exotic magnetic ground state is rare-earth pyrochlore oxides, $\text{R}_2\text{B}_2\text{O}_7$, where R^{3+} and B^{4+} are generally trivalent rare-earth and tetravalent transition-metal ions, respectively. In this rare-earth magnet family, the ground state of some Kramers ion is a well-separated crystal electric field doublet with interacting $J_{\text{eff}} = 1/2$ pseudo-spins at low temperatures. Depending upon how the ground state doublet transforms under time-reversal symmetry and local D_{3d} crystal field symmetry of the rare-earth site, this pyrochlore can harbor dipole-octupole ground state doublet, which supports exotic $\text{U}(1)$ quantum spin liquid ground state [32, 33]. For example, in the quantum spin liquid candidate $\text{Ce}_2\text{Zr}_2\text{O}_7$, x and z components of pseudo-spin-1/2 degrees of freedom of Ce^{3+} ion behave as dipoles, whereas only the y component behaves as an octupole under the time-reversal symmetry and lattice symmetry [33]. Coupling between magnetic field and spinons enables to control spinon excitations by applying an external magnetic field in this octupolar spin liquid candidate [32]. Among 3D spin liquid candidates, three-dimensional network of corner-sharing triangles known as hyperkagome

* pkhuntia@iitm.ac.in

lattice has recently drawn significant attention due to their rich ground state properties. One exemplar is $\text{PbCuTe}_2\text{O}_6$, wherein spin $S = 1/2$ transition metal Cu^{2+} ions constitute a hyperkagome lattice. The local probe techniques nuclear magnetic resonance (NMR) and muon spin resonance (μSR) revealed a dynamic ground state down to 20 mK in this hyperkagome [24, 25]. Diffusive continua in magnetic excitation spectra revealed by neutron scattering experiment provides a strong evidence of fractional spinon excitations in this 3D frustrated magnet [26]. Another geometrically frustrated effective spin $J_{\text{eff}} = 1/2$ 3D spin liquid candidate is $\text{Na}_4\text{Ir}_3\text{O}_8$ [34, 35]. Despite strong antiferromagnetic interaction between Ir^{4+} ($J_{\text{eff}} = 1/2$) moments, which was confirmed by a large Curie-Weiss temperature of -650 K, there is no sign of magnetic ordering down to a few Kelvin. A theoretical study proposed the existence of a Z_2 quantum spin liquid state in the quantum regime (i.e, small spin) of hyperkagome lattice $\text{Na}_4\text{Ir}_3\text{O}_8$ [36]. However, a small splitting of zero field cooled and field cooled magnetization data suggests the role of static moments below 7 K, which imposes a strong constraint for the unambiguous identification of spin liquid ground state in this material [37]. The rare realization of 3D QSL is due to the fact that the Néel order or spin freezing is energetically favorable over the QSL state in the case of a 3D frustrated spin-lattice for $S > 1/2$. However, frustration induced strong quantum fluctuations in the $S = 1/2$ or $J_{\text{eff}} = 1/2$ system makes it a potential candidate to host a dynamic ground state [5, 30, 38]. It is highly relevant to explore whether the disorder interaction or exchange anisotropy or lattice imperfections account for spin-freezing in this type of 3D spin liquid candidates.

In this context, synthesis and investigation of new three-dimensional frustrated spin-lattices, wherein interplay between competing degrees of freedom and spin correlations could lead to exotic quantum states, are highly needed. Considerable efforts have been devoted in this direction, for instance, disorder-free $4f$ -based hyperkagome lattice, wherein spin frustration and anisotropic interactions governed by spin-orbit interaction stabilizing an effective low energy $J_{\text{eff}} = 1/2$ ground state, offers an alternate route for the realization of elusive 3D spin-liquids. Hyperkagome lattice-based material $\text{Li}_3\text{Yb}_3\text{Te}_2\text{O}_{12}$ wherein Yb^{3+} spins decorated on a corner-shared frustrated triangular network shows a dynamical ground state down to 38 mK temperature [39]. Magnetic Yb^{3+} ions show short-range spin correlations with $J_{\text{eff}} = 1/2$ degrees of freedom in the ground state. One promising family of compound to study rare-earth hyperkagome lattice is lanthanide garnets with general formula $\text{R}_3\text{A}_2\text{X}_3\text{O}_{12}$, R = rare-earth elements; A = Ga, Sc, In, Te; X = Ga, Al, Li [40]. In this series, rare-earth ions occupying two interpenetrating frustrated hyperkagome networks have a rich potential to harbor myriads of novel physical phenomena. For example, antiferromagnetic spin correlation and local magnetic anisotropy lead to a non-trivial magnetic structure with long-range hidden order state in $\text{Gd}_3\text{Ga}_5\text{O}_{12}$ [41, 42]. Spin clusters behave like a single object due to strong spin correlation and these spin clusters show long-range non-dipolar order although the individual

spin maintains a dynamic liquid-like state [41, 43]. On the other hand, emergent magnetic behavior with short-range spin correlations was observed in $J_{\text{eff}} = 1/2$ Yb^{3+} containing garnet $\text{Yb}_3\text{Ga}_5\text{O}_{12}$ [44]. The specific heat data show a λ -like anomaly which was attributed to long-range magnetic order [45]. However, muon spin resonance and Mössbauer spectroscopy measurements indicate the absence of long-range magnetic order [45, 46]. In an opposite scenario, antiferromagnetically ordered state develops below in the sub-Kelvin temperature range in other members of the garnet family [47, 48]. Though there are several studies on gallium garnets, magnetic properties of scandium gallium garnets have yet to be investigated so far. Recent study on $\text{R}_3\text{Sc}_2\text{Ga}_3\text{O}_{12}$ (R = Tb, Dy, Ho) reveals that most of these garnets undergo a long-range antiferromagnetic ordering state at low temperature [40]. The magnetic properties of this family of materials is highly sensitive to external stimuli such as chemical pressure, temperature, or an applied magnetic field. It is pertinent to test the effect of external perturbations such as non-magnetic or magnetic ions on the anisotropy, exchange interactions and hence the underlying spin Hamiltonian in this interesting class of three-dimensional frustrated magnets. The magnetic moment of Yb^{3+} ion is relatively weak compared to other R^{3+} ions. Being a Kramers ion Yb^{3+} , a combination of crystal electric field and spin-orbit coupling could lead to a low energy $J_{\text{eff}} = 1/2$ state in the Yb variant of this promising garnet series. This suggests that $\text{Yb}_3\text{Sc}_2\text{Ga}_3\text{O}_{12}$ is of special interest to look for spin-orbit driven ground state.

Herein, we report the synthesis, magnetization, electron spin resonance (ESR), and thermodynamic studies on a garnet $\text{Yb}_3\text{Sc}_2\text{Ga}_3\text{O}_{12}$, wherein Yb^{3+} ions constitute a three-dimensional frustrated corner-sharing network of triangles, namely, a hyperkagome spin-lattice. The combination of crystal electric field and spin-orbit coupling stabilizes a low energy pseudo-spin $J_{\text{eff}} = 1/2$ state of the Kramers doublets of Yb^{3+} ion at low temperature. The absence of ZFC-FC splitting of magnetic susceptibility in 0.001 T rules out spin-freezing down to 1.8 K in this material. The low-temperature Curie-Weiss fit yields a weak antiferromagnetic interaction between Yb^{3+} ($J_{\text{eff}} = 1/2$) moments in the spin-lattice. The magnetic ground state is investigated via thermodynamic measurements which reveal that this garnet remains in a quantum disordered ground state at least down to 130 mK. The specific heat in zero field shows a broad maximum around 200 mK implying the presence of short-range spin correlations in this three-dimensional frustrated spin-lattice. The crystal electric field calculations infer that the lowest Kramers ground state is well separated from the excited states and imply considerable magnetic anisotropy which is consistent with experiments.

II. EXPERIMENTAL DETAILS

Polycrystalline sample of $\text{Yb}_3\text{Sc}_2\text{Ga}_3\text{O}_{12}$ was prepared via the sol-gel method. Rare-earth oxide Yb_2O_3 was preheated at 900°C for 6 hours prior to use to remove moisture and carbonates. Stoichiometric amount of Yb_2O_3 (Alfa Aesar,

99.998%), Sc_2O_3 (Alfa Aesar, 99.9%) and Ga_2O_3 (Alfa Aesar, 99.999%) were dissolved in hot nitric acid separately in three beakers. The concentration of these acidic solutions was reduced by adding and evaporating deionized water. These three nitrate solutions were then mixed together and polyethylene glycol was added to the solution. This solution was kept in between 90°C to 120°C on a magnetic stirrer for several hours. The gel was dried yielding ash-like powders, which were preheated at 800°C for 6 hours, and finally a white color polycrystalline sample was obtained. This is followed by the heat treatment of the resulting sample at 1000°C , 1100°C and 1200°C for a few days. Before each heat treatment, the sample was grounded and pelletized to ensure better homogeneity. Rigaku x-ray diffractometer was deployed to check the phase purity at room temperature using $\text{Cu } K_\alpha$ radiation. Quantum Design, SQUID-VSM was used to perform magnetization measurements in the temperature range $1.8 \text{ K} \leq T \leq 350 \text{ K}$ under magnetic field $0 \text{ T} \leq \mu_0 H \leq 5 \text{ T}$. Electron spin resonance (ESR) experiments were performed at 9.4 GHz (X-band frequency) on a high quality polycrystalline sample of $\text{Yb}_3\text{Sc}_2\text{Ga}_3\text{O}_{12}$ material for temperatures down to 4 K. Specific heat measurements were carried out with a Quantum Design, Physical Properties Measurement System (QD, PPMS) in magnetic fields up to 7 T and in the temperature range $1.8 \text{ K} \leq T \leq 200 \text{ K}$. The low-temperature specific heat measurement down to 130 mK was performed using a dilution refrigerator set up attached to the Dynacool PPMS from Quantum Design, USA. Fitting and modeling of the crystal-electric-field (CEF) effects were preformed using PHI software[49].

A. Crystal structure

For the Rietveld refinement of $\text{Yb}_3\text{Sc}_2\text{Ga}_3\text{O}_{12}$ hyperkagome material, initial crystallographic parameters were taken from its iso-structural compound $\text{Gd}_3\text{Sc}_2\text{Ga}_3\text{O}_{12}$ which crystallizes in the cubic space group $Ia\bar{3}d$ [40]. Rietveld refinement was performed using FullProf Suite on powder XRD data recorded at room temperature and the refined parameters are $R_p = 8.3\%$, $R_{wp} = 9.2\%$ and $\chi^2 = 5.4$ [50] (see Fig. 2). Refined atomic coordinates are presented in Table I. The lattice constant a turned out to be 12.391 \AA , which is smaller than that found in other rare-earth-based iso-structural compounds ($\text{R}_3\text{Sc}_2\text{Ga}_3\text{O}_{12}$, $\text{R} = \text{Gd}, \text{Tb}, \text{Dy}$ and Ho) [40]. This reduction is due to the small ionic radius of Yb^{3+} ion compared to other rare-earth ions. A tiny impurity peak at around $2\theta \approx 31^\circ$ indicates a minor (1.5%) phase of unreacted Sc_2O_3 which is non-magnetic and its impact on the overall magnetic behavior of the oxide is negligible. The crystal structure was drawn by using VESTA, which is shown in Fig. 1a [51]. The two inter-penetrating hyperkagome network build up of Yb^{3+} ions is shown in Fig. 1b. Each Yb atom is surrounded by eight oxygen atoms forming a YbO_8 polyhedron. Four of them are at a distance 2.4 \AA and the rest are at 2.455 \AA forming a dodecahedron structure. The nearest-neighbor Yb–Yb bond length is 3.794 \AA , whereas the second nearest-neighbor bond is 5.796 \AA . There

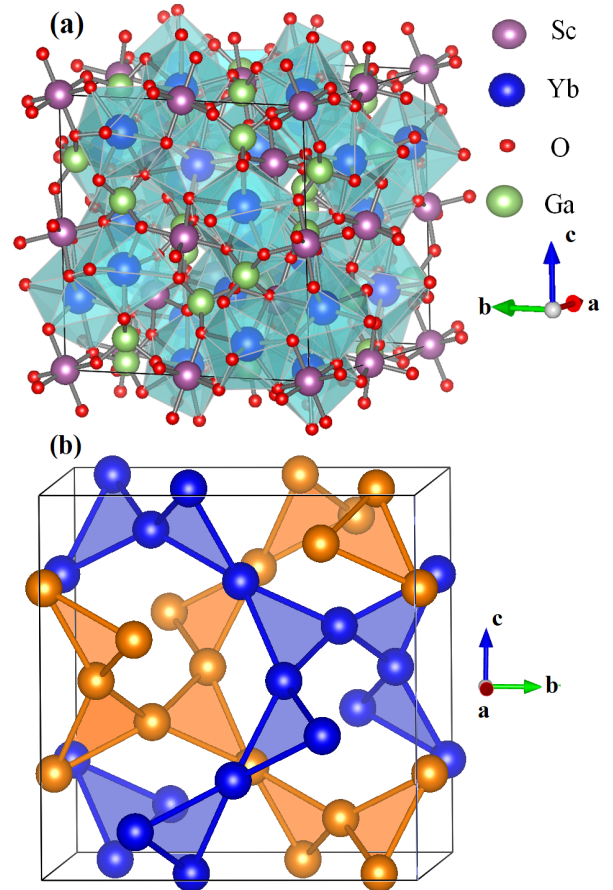


FIG. 1. (a) Crystal structure of $\text{Yb}_3\text{Sc}_2\text{Ga}_3\text{O}_{12}$. (b) Two interpenetrating hyperkagome network of Yb^{3+} ions.

are two Yb–O–Yb bridging exchange paths between two nearest-neighbor Yb atoms both making an angle 102.8° . The presence of corner-shared triangles might induce magnetic frustration in this material.

TABLE I. Structural parameters of $\text{Yb}_3\text{Sc}_2\text{Ga}_3\text{O}_{12}$ determined from the Rietveld refinement of powder x-ray diffraction pattern taken at room temperature using Fullprof software. Space group $Ia\bar{3}d$ and cell parameters $a = b = c = 12.391 \text{ \AA}$, $\alpha = \beta = \gamma = 90^\circ$, $\chi^2 = 5.4$.

Atoms	Wyckoff	x	y	z	Occ.
Ga	24d	0	0.25	0.375	1
Sc	16a	0	0	0	1
Yb	24c	0	0.25	0.125	1
O	96h	-0.0316	0.0561	0.1508	1

B. Magnetization

Magnetic susceptibility measurements were carried out in the temperature range $1.8 \text{ K} \leq T \leq 350 \text{ K}$ under several

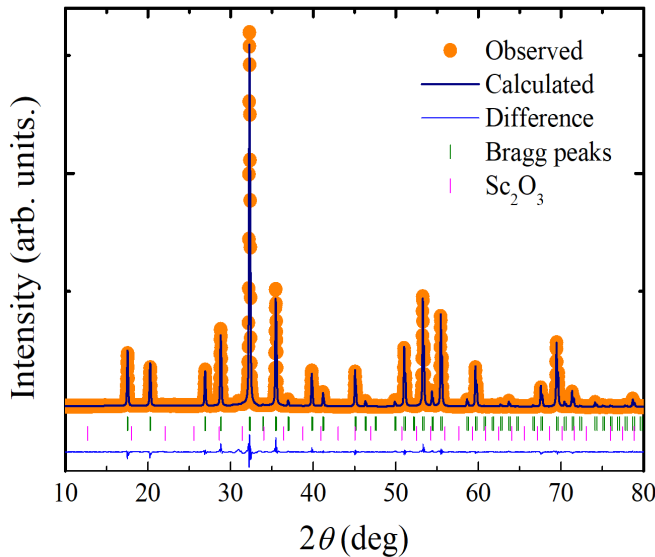


FIG. 2. Rietveld refinement of powder XRD data taken at room temperature.

applied magnetic fields. Fig. 3a represents the temperature dependence of magnetic susceptibility data taken in applied magnetic fields ranging from 0.01 T $\leq T \leq 5$ T. The absence of an anomaly in magnetic susceptibility data indicates that there is no magnetic phase transition down to 1.8 K. The absence of any splitting in zero field cooled (ZFC) and field cooled (FC) data taken in 0.001 T rules out spin freezing down to 1.8 K (see Fig. 3b). This is further confirmed by the absence of hysteresis in the magnetization isotherm taken at 1.8 K (see Supplementary Fig.1b). High temperature inverse susceptibility data were well reproduced using the Curie-Weiss formula, $\chi(T) = \frac{C}{T - \theta_{\text{CW}}}$ in the temperature range 200 K $\leq T \leq 350$ K (see Fig. 3c). The fit yields a negative $\theta_{\text{CW}} \approx -114 \pm 1$ K, which is attributed to crystal electric field effects and a change in the population of crystal electric field levels can induce a strong curvature in $\chi^{-1}(T)$ curve (here below 150 K). The Curie-Weiss constant C turns out to be 2.49 cm³·K/mol resulting in effective moment $\mu_{\text{eff}} = 4.5 \mu_{\text{B}}$, close to the free ion effective moment (4.54 μ_{B}) of Yb³⁺ ($4f^{13}$, $^2F_{7/2}$; $J = 7/2$) ion ($g\sqrt{J(J+1)}\mu_{\text{B}}$, g -Landé factor). In the presence of crystal electric field (CEF), the eight-fold degenerate ground state of Yb³⁺ ion splits into four Kramers doublets [52]. In this scenario, Curie-Weiss temperature obtained from high temperature fit is inadequate to describe the magnetic exchange interaction as some of the Kramers doublets with higher energy might be populated and Curie-Weiss temperature is dominated by these crystal field levels (see Supplementary text). The deviation of the temperature dependence of inverse magnetic susceptibility around 150 K indicates the presence of another energy scale of interaction between Yb³⁺ moments at low temperature. In principle, the correlation between $4f$ moments develop at very low temperature and this correlations accompanied by competing degrees of freedom account for the ground state properties in rare-earth-based frustrated quantum magnets

[23]. In order to get an idea regarding the exchange interaction between Yb³⁺ moments, we have fitted the temperature dependence of inverse magnetic susceptibility with Curie-Weiss formula in the temperature range 1.8 $\leq T \leq 10$ K (see Fig. 3c). A weak Curie-Weiss temperature of $-0.2(1)$ K and an effective moment of 2.9(3) μ_{B} were obtained from the best fit (see Supplementary Fig. 1a). The negative and small Curie-Weiss temperature indicates the presence of weak antiferromagnetic interaction between the Yb³⁺ spins. Small Curie-Weiss temperature is usually found in rare-earth magnets [23, 44, 53]. From the value of the effective moment, the g factor turns out to be 3.3(3). The reduced effective moment compared to that expected for Yb³⁺ free ion is attributed to the $J_{\text{eff}} = 1/2$ Kramers doublet ground state at low temperatures [23, 53–55]. Fig. 3d depicts

TABLE II. Comparison of lattice parameter, Curie-Weiss temperature (θ_{CW}), ordering temperature of scandium garnet R₃Sc₂Ga₃O₁₂.

R	Gd	Tb	Dy	Ho	Yb
a (Å)	12.573	12.539	12.502	12.475	12.391
θ_{CW} (K)	-2.2	-1.2	-0.8	-2.9	-0.2(1)
T_{N} (K)	<0.4	0.7	1.11	2.4	<0.13
Reference	[40]	[40]	[40]	[40]	This work

the magnetization isotherms at different temperatures. In higher field and low temperature, magnetization increases linearly due to the Van-Vleck paramagnetism. From the linear behavior of the curve, we have determined a Van-Vleck term of $\chi_{\text{VV}} = 0.0059 \mu_{\text{B}}/\text{T} = 0.003 \text{ cm}^3/\text{mol}$. The saturation magnetic moment was found to be 1.43 $\mu_{\text{B}}/\text{Yb}^{3+}$ after subtracting the Van Vleck term, which is consistent with $M_{\text{s}} = g_{\text{avg}}J_{\text{eff}}(1/2)\mu_{\text{B}}$. The fit of the $M(H)$ data taken at 1.8 K with Brillouin function also yields a g value of $\approx 3.0(2)$ close to the value obtained from Curie-Weiss fit to low-temperature inverse magnetic susceptibility data (see Fig. 3d). However, the Brillouin fit deviates slightly, probably indicating the presence of a weak antiferromagnetic interactions between Yb³⁺ moments at low temperature. The data taken at 20 K are well fitted with the Brillouin function as the material is in the paramagnetic region. In these fittings, the J value was fixed to 1/2 to account for the $J_{\text{eff}} = 1/2$ ground state. The dipolar interaction energy and dipolar Curie-Weiss temperature were deduced from the formula $E_{\text{d}} = \left(\frac{8}{\sqrt{6}}\right)^3 \frac{(g\mu_{\text{B}}S)^2}{a^3}$ and $\theta_{\text{CW}}^{\text{dip}} = 32\pi \frac{(g\mu_{\text{B}})^2 S(S+1)}{3a^3 k_{\text{B}}}$ which was used for the isostructural compound Yb₃Ga₅O₁₂ [55]. Here a is the lattice parameter. E_{d} and $\theta_{\text{CW}}^{\text{dip}}$ are turned out to be 31 mK and 90 mK, respectively. Different magnetic interactions contributes additively to the Curie-Weiss temperature (i.e, $\theta_{\text{CW}} = \theta_{\text{CW}}^{\text{dip}} + \theta_{\text{CW}}^{\text{ex}}$) [56, 57], the Curie-Weiss temperature due to exchange interaction (i.e, $\theta_{\text{CW}}^{\text{ex}}$) turned out to be $\sim -0.3(1)$ K. The exchange interaction J_{ex} could be obtained using the formula $J_{\text{ex}} = \frac{3k_{\text{B}}\theta_{\text{CW}}^{\text{ex}}}{zS(S+1)}$ [58], where z represents the number of nearest-neighbors. Using $z = 4$ for hyperkagome structure and

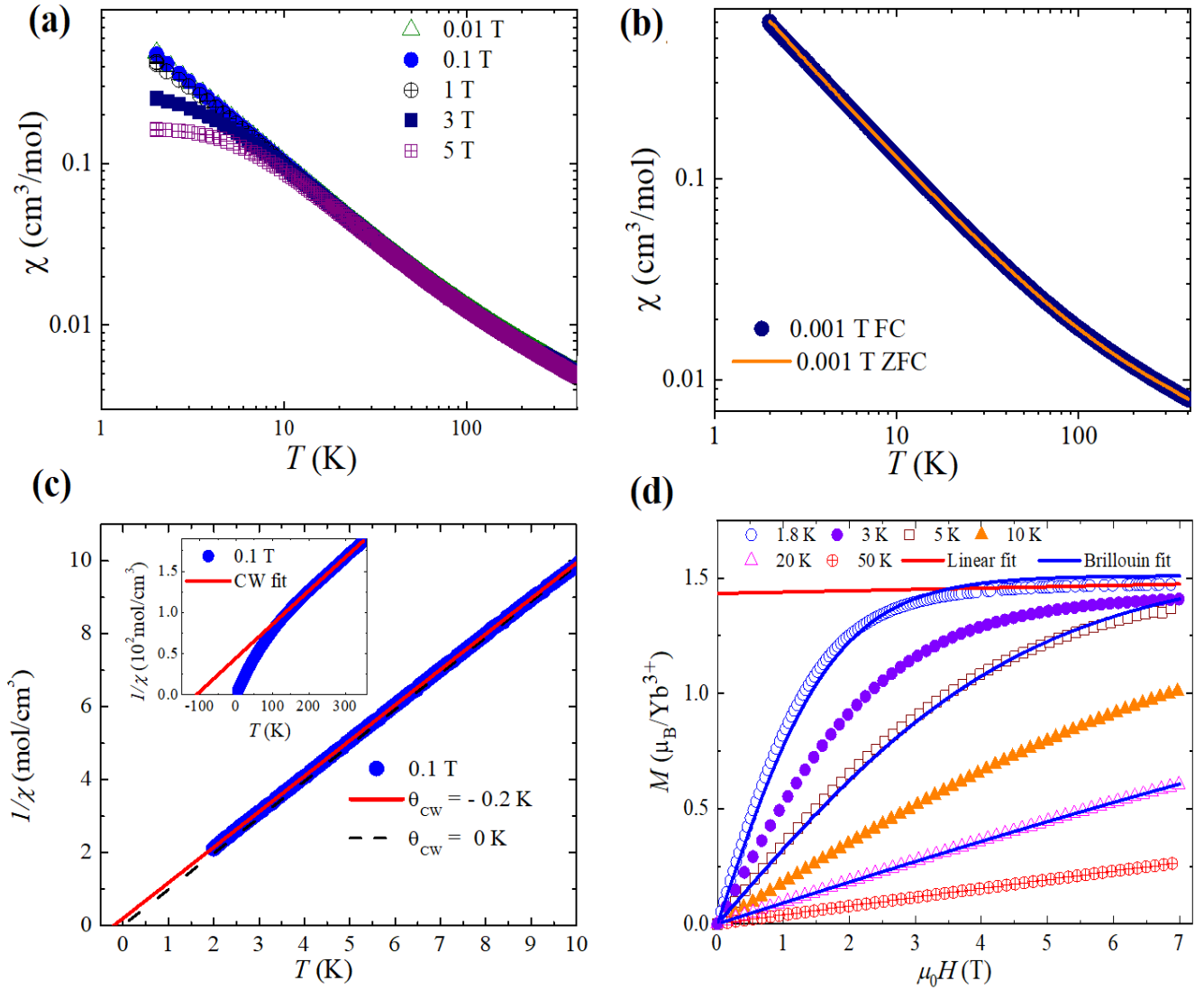


FIG. 3. (a) The temperature dependence of magnetic susceptibility in different applied magnetic fields reordered in ZFC mode. (b) The temperature dependence of zero field cooled and field cooled magnetization data taken in 0.001 T. (c) Curie-Weiss fit to inverse susceptibility data taken in 0.1 T. Blue filled circle denotes experimental data, whereas solid and dashed lines denote Curie-Weiss fits. Inset shows the same fit at higher temperature range $200 \text{ K} \leq T \leq 350 \text{ K}$. (d) Magnetic isotherms at different temperatures. Magnetization taken in ramping up and down modes remain identical that add further credence to the absence of spin glass physics. From the slope of linear fit (solid red line) to high field data taken at 1.8 K a Van Vleck contribution to susceptibility was extracted. Blue lines are Brillouin fits for $J_{\text{eff}} = 1/2$ at different temperatures.

effective spin $S \equiv J_{\text{eff}} = 1/2$, we found $J_{\text{ex}} = -0.3(1) \text{ K}$. The presence of weak exchange interaction is usual in rare-earth oxides which is attributed to the fact that the $4f$ orbitals of rare-earth ions are localized and well shielded yielding weak overlap between two nearest-neighbor orbitals.

C. Electron Spin Resonance (ESR)

Electron spin resonance (ESR) is an excellent low energy, local probe to determine the effective g -factor as well as characterizing single-ion and exchange anisotropies, which

are crucial to establish realistic microscopic Hamiltonian of frustrated quantum materials. It was shown that ESR can shed microscopic insights into the QSL state and associated exotic excitations in frustrated magnets with significant spin-orbit interaction [59]. Fig. 4 depicts ESR signals of a polycrystalline sample of $\text{Yb}_3\text{Sc}_2\text{Ga}_3\text{O}_{12}$ at representative temperatures. Due to the rather large linewidth, Yb containing secondary phases may be excluded as origin of the signal. We described the line by a Lorentzian shape including also the negative resonance field component due to the influence of the counter-rotating component of the linearly polarized microwave field. Such a fit yields for the 20 K data a

resonance field of 0.18 T (which corresponds to a g -value of 3.6) and a linewidth of 0.2 T. The large line width as compared to the resonance field pose a strong constraint to precisely quantify temperature dependencies of ESR parameters in the measured temperature range $4 \leq T \leq 175$ K. Nevertheless, a clear tendency of line broadening towards low and high temperatures as well as a down shift of the resonance field towards low temperature can be identified. This behavior may be due to a relaxation via the first excited crystal electric field level of the Yb^{3+} ion and the slowing down of Yb^{3+} spin fluctuations in the low temperature regime [60]. The strong deviation from a symmetric Lorentzian line shape points to off-diagonal terms in the dynamic susceptibility. This is typical for systems with anisotropic spin lattices and becomes even more pronounced when very broad lines are present [61]. A detailed discussion in this direction would be reasonable only if ESR data of single crystals would be available.

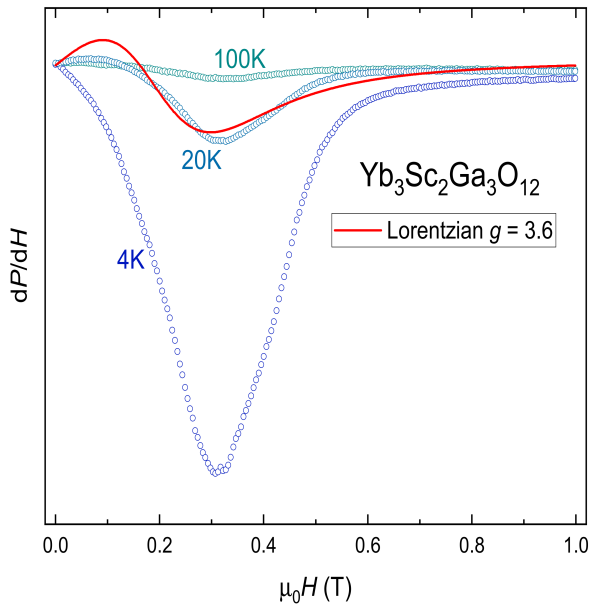


FIG. 4. ESR spectra of a polycrystalline sample of $\text{Yb}_3\text{Sc}_2\text{Ga}_3\text{O}_{12}$ at indicated temperatures and X-band frequency. dP/dH denotes the first field derivative of the absorbed microwave power. Line denotes fitting of the 20 K data with a Lorentzian shape with a corresponding g -value of 3.6.

D. Specific heat

Specific heat provides an excellent probe to gain insights into the ground state properties of this rare-earth hyperkome lattice. Fig. 5a shows the specific heat as a function of temperature down to 130 mK in zero field. The absence of any anomaly in zero field, thus confirms the evasion of long-range magnetic ordering down to at least 130 mK despite a weak antiferromagnetic exchange interaction between $J_{\text{eff}} = 1/2$ moments. The peak in specific heat due to the nuclear Schottky effect usually occurs below 10^{-2} K [62–64]. To calculate the expected nuclear specific heat contribution, we

have considered the fact that the natural abundance of ^{171}Yb ($I = 1/2$) and ^{173}Yb ($I = 5/2$) are 14.31% and 16.13%, respectively (see Fig. 5a) [65–67]. The energy separation between two consecutive levels for ^{171}Yb and ^{173}Yb , are 63.9 mK and 17.55 mK, respectively, which are taken from that reported for the isostructural compound $\text{Yb}_3\text{Ga}_5\text{O}_{12}$ [65]. The quadrupole coupling constant P (see supplementary equation 3) is zero for ^{171}Yb and non-zero for ^{173}Yb . However, we have neglected the quadrupole term in our calculation (see SI for details) due to its insignificant impact on shifting the Schottky peak. Upon the application of an external magnetic field, a broad maximum appears at low temperature in specific heat data of $\text{Yb}_3\text{Sc}_2\text{Ga}_3\text{O}_{12}$, that shifts significantly to higher temperature upon increasing magnetic field (see Fig. 5b), which is associated with the electronic Schottky anomaly originating from the Zeeman splitting of the lowest lying energy levels. To evaluate Schottky contribution, field dependent $C_p(H)$ data were fitted with the equation $C_p = C_L + C_S(\Delta)$ (see Fig. 5c), where $C_S(\Delta)$ is the specific heat with energy level splitting Δ due to an applied magnetic field $\mu_0 H$ [68, 69]. C_L is the lattice contribution to the specific heat. We have fitted the low-temperature zero-field specific heat data in the temperature range $4 \text{ K} \leq T \leq 22 \text{ K}$ with the equation relevant for lattice specific heat in the simplest approximation

$$C_L = \alpha T^3 \quad (1)$$

and then extrapolated it to lower temperature. The Schottky specific heat $C_S(\Delta)$ is given by

$$C_S(\Delta) = 3fR \left(\frac{\Delta}{k_B T} \right)^2 \frac{\exp\left(\frac{\Delta}{k_B T}\right)}{\left[1 + \exp\left(\frac{\Delta}{k_B T}\right) \right]^2}. \quad (2)$$

The factor 3 indicates that there are 3 Yb ions in a formula unit. Here, f denotes the fraction of Yb^{3+} spins participating in the splitting of the ground state. This value is close to one ($f > 0.9$ for fields $\mu_0 H > 3$ T) indicating that almost all the spins are contributing to the specific heat. It is worth mentioning that, for transition metal oxides, f denotes the fraction of orphan or defect spins (5-10 %) that are present in the system owing to disorder [12, 70]. It is found that the value of Δ increases with an external applied magnetic field typical for many frustrated magnetic materials [39, 64]. The Landé- g factor turns out to be 3.3(1) from the slope of the linear fit to Δ/k_B vs. $\mu_0 H$ plot (see inset of Fig. 5c), which is consistent with the result obtained from magnetization data. We get a small zero-field splitting of 0.2(1) K from the intercept of the extrapolated linear fit. However, the deviation of the zero field data from Schottky specific heat indicates that the peak around 200 mK might be due to the presence of short-range spin correlation between Yb^{3+} ions in this 3D spin-lattice. It is worthwhile to mention that a crystal electric field can also split the energy levels and give rise to Schottky type anomaly. However, the energy difference from the ground state to the first excited state in most of the rare-earth materials is of the order of 5 meV or more, which corresponds to a temperature of 58 K [23, 47, 71, 72]. Magnetic specific

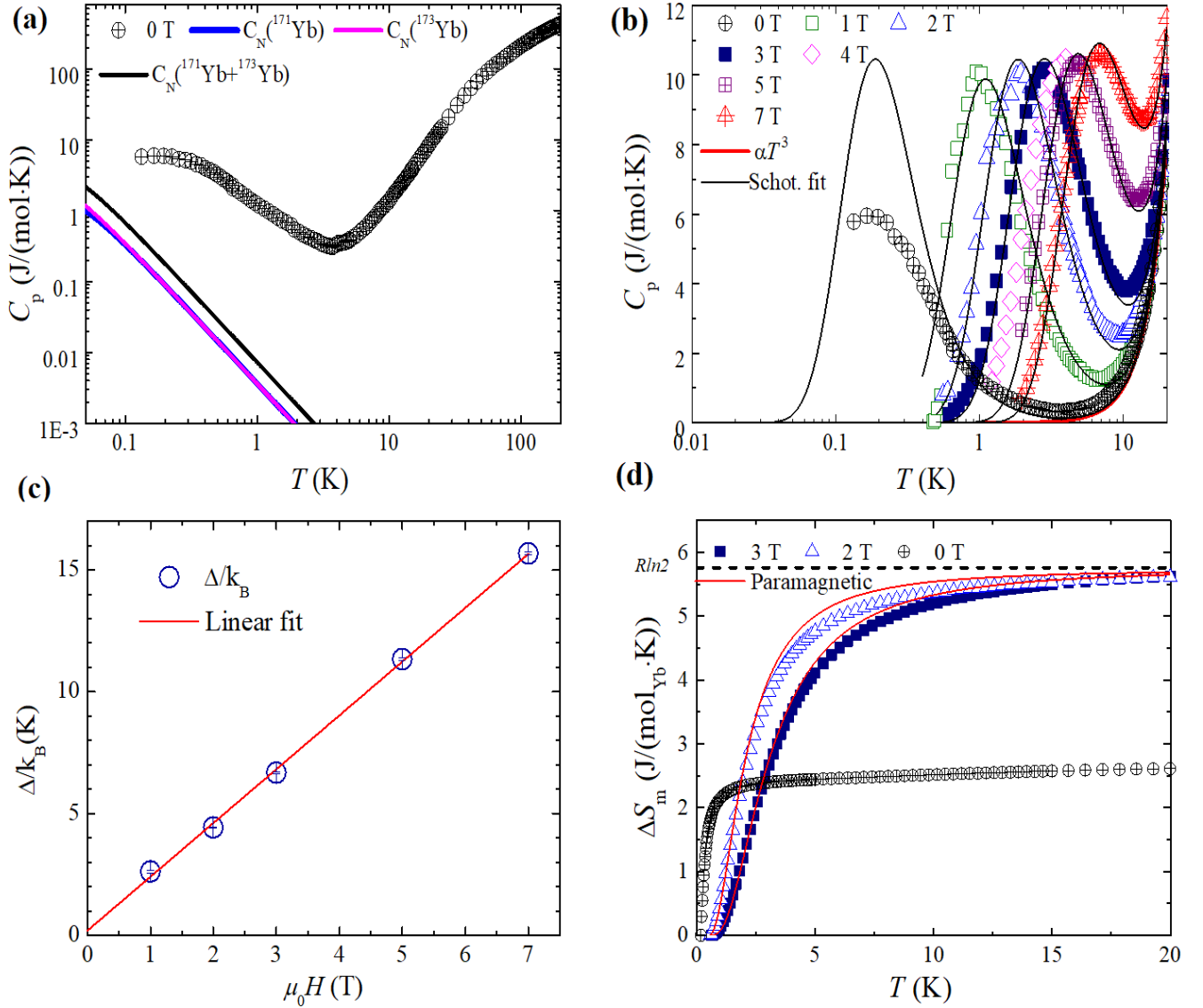


FIG. 5. (a) Temperature dependence of specific heat ($130 \text{ mK} \leq T \leq 200 \text{ K}$) for $\text{Yb}_3\text{Sc}_2\text{Ga}_3\text{O}_{12}$ in zero field. Nuclear Schottky contribution to the specific heat for $3 \times 0.1431 \text{ mol}$ of ^{171}Yb and $3 \times 0.1613 \text{ mol}$ of ^{173}Yb are denoted by blue and pink line, respectively. (b) Low temperature specific heat ($130 \text{ mK} \leq T \leq 20 \text{ K}$) in several applied magnetic fields. Corresponding Schottky fits are denoted by black solid lines. Phonon contributions were taken into account while fitting by adding αT^3 term indicated by red solid line. (c) Linear behavior of Schottky gap (Δ/k_B) with applied magnetic field and the solid red line is a linear fit. From the slope of the fit we found $g = 3.3(1)$ and the intercept turns out to be $0.2(1) \text{ K}$. (d) Magnetic entropy in applied magnetic fields. Corresponding paramagnetic entropy in applied fields are denoted by red solid lines. Experimental entropy is slightly smaller than the ideal paramagnet which suggests the existence of small exchange interaction and/or magnetic frustration. For higher fields, it saturates at 97 % of the full entropy ($R \ln 2$) expected for magnetic materials with $J_{\text{eff}} = 1/2$ degrees of freedom consistent with magnetization results.

heat C_m was obtained after subtracting the lattice (C_L) and nuclear contribution [$C_N(^{171}\text{Yb} + ^{173}\text{Yb})$] to specific heat from the raw specific heat data C_p in the entire temperature range. However, we did not subtract the nuclear contribution for higher field data as our lowest accessible temperature in applied field is 0.5 K , where the nuclear contribution is almost negligible [i.e., $0.026 \text{ J}/(\text{mol}\cdot\text{K})$]. The magnetic entropy can shed insights into the ground state properties of frustrated magnetic materials. We have extracted the entropy by integrating C_m/T from the lowest accessible temperature

(130 mK for zero field) to 20 K and the results are shown in Fig. 5d. Due to experimental limitations in accessing temperature below 130 mK , the zero field specific heat is not fully recovered yielding a lower value of entropy than that expected for spin half magnetic materials. The zero-field entropy does not saturate to $R \ln 2$ even up to 20 K . This residual entropy below 130 mK might indicates the role of magnetic frustration at very low temperature. However, in the application of a magnetic field, the entropy is dominated by the Schottky effect in Kramers doublet systems. The obtained

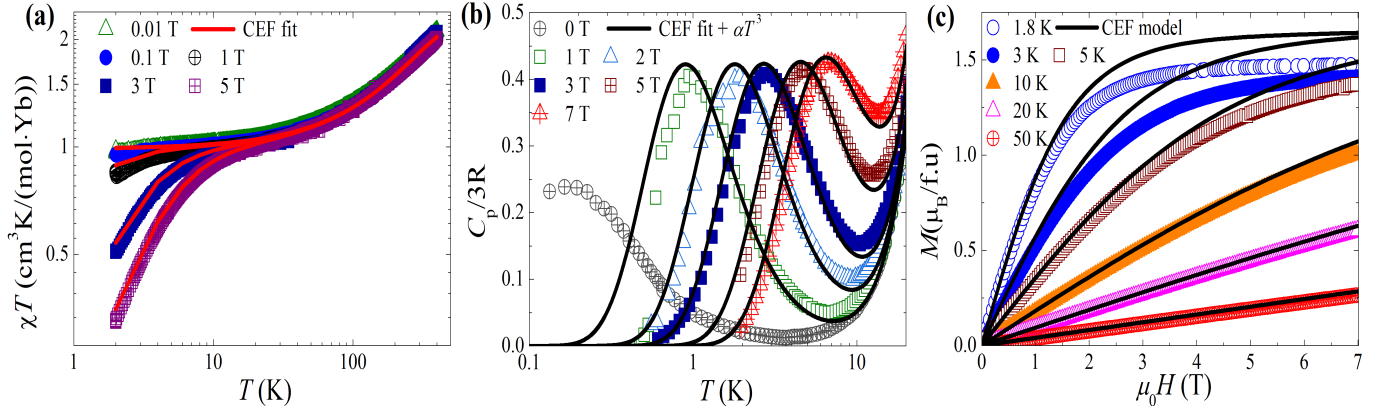


FIG. 6. (a) The temperature dependence of χT emphasizing the χ behavior at low temperatures. (b) The temperature dependence of specific heat measured in different magnetic fields. (c) Magnetization as a function of external magnetic field at several temperatures. Lines correspond to the CEF model presented in the text.

TABLE III. CEF parameters (in meV) for CEF Hamiltonian of Eq. (3) and g factors of the ground state for the CEF model.

B_2^0	B_2^2	B_4^0	B_4^2	B_4^4	B_6^0	B_6^2	B_6^4	B_6^6	g_x	g_y	g_z
-0.06229	0.3036	0.08183	-0.04343	-0.03914	0.0000166	-0.01486	0.02468	-0.009285	2.93	2.25	4.24

high temperature θ_{CW} (-114 K), which indicates crystal field splitting of the ground state, is very large. We expect that the excited state doublets are well separated from the ground state so that we can describe the low-temperature properties by accounting only the lowest $J_{\text{eff}} = 1/2$ ground state. The entropy taken in 3 T saturates with a value 5.6 J/(mol·K) which is close to the full entropy of $R \ln 2$ [i.e., 5.76 J/(mol·K)] for $J_{\text{eff}} = 1/2$ spin state. This suggests that the ground state of this three-dimensional spin-lattice could be mapped with a low energy effective $J_{\text{eff}} = 1/2$ state at low temperature, which is consistent with magnetization results [73, 74].

E. Crystal electric field (CEF) calculations

We performed a combined fit of specific heat data measured in 1, 2, 3, 5, and 7 T as well as magnetic susceptibility data measured in 0.01, 0.1, 1, 3, and 5 T. According to the Hund's rule, the ground state multiplet of the Yb^{3+} ion is $^2F_{7/2}$, which is in a crystal field split into four Kramers doublets composed of $|\pm m_j\rangle$ states [$m_j = (2n - 1)/2$, where $n = 1-4$]. The composition of the four Kramers doublets directly depends on the CEF Hamiltonian, which can be written as

$$H_{\text{CEF}} = \sum_{i,j} B_j^i O_j^i, \quad (3)$$

where O_j^i are Stevens operators [75] and B_j^i are the corresponding scaling parameters. The relevant B_j^i (Table III) are determined by point symmetry at the Yb^{3+} site and in general comply with those determined for the isostructural compound $\text{Yb}_3\text{Ga}_5\text{O}_{12}$ [76]. Indeed, we obtained a very good agreement with the data measured in the applied

TABLE IV. CEF energy levels (in meV) for the CEF model.

E_0	E_1	E_2	E_3
0	69	96	143

magnetic field [lines in Fig. 6(a) and (b)] for the derived CEF parameters (Table III), when considering additional T^3 term for the specific heat, accounting for the phonon contribution at low temperatures. Finally, we have calculated the corresponding magnetization curves $M(H)$ [lines in Fig. 6(c)]. The agreement of the simulation and experiment is quite reasonable for both experiments. The derived magnetic anisotropy of the CEF ground state is determined by the g factor, also given in Table III, implying a rather uniaxial anisotropy, as g_z is considerably larger than g_x and g_y . In fact, the derived g values are in agreement with the average $g = 3.6$ derived from the ESR data measured at 20 K. All energy levels are summarized in table Table IV, indicating that the ground state is well separated from the excited states, as found also in $\text{Yb}_3\text{Ga}_5\text{O}_{12}$ [76]. We note that, the broad maximum in specific heat around 200 mK in zero field is clearly not related to CEF effects and as suggested above most likely associated with the presence of short-range spin correlations.

III. DISCUSSION

The intertwining of spin-orbit coupling and electron correlation in frustrated magnets can stabilize exotic quantum states. In this context, rare-earth-based $4f$ frustrated magnets offer an exciting platform. In these materials, anisotropy

and crystal electric field generated by the neighboring ligands govern the ground state properties. The choice of a suitable chemical element has a great role in tuning the crystal electric field, anisotropy and exchange interaction and hence the ground state properties of rare-earth-based frustrated magnet. The hyperkagome material $\text{Yb}_3\text{Sc}_2\text{Ga}_3\text{O}_{12}$ belongs to the garnet family with cubic space group $Ia\bar{3}d$ and lattice constant $a = 12.391 \text{ \AA}$. Unlike $\text{R}_3\text{Sc}_2\text{Ga}_3\text{O}_{12}$ garnets ($\text{R} = \text{Tb}, \text{Dy}, \text{Ho}$), which orders at low temperature, $\text{Yb}_3\text{Sc}_2\text{Ga}_3\text{O}_{12}$ does not show any long-range magnetic ordering at least down to 130 mK. This might be due to the low magnetic moment of Yb^{3+} and low exchange energy compared to other $\text{R}_3\text{Sc}_2\text{Ga}_3\text{O}_{12}$ compounds [40]. Furthermore, the absence of ZFC-FC splitting rules out spin-freezing in this material. The small negative Curie-Weiss temperature indicates the presence of a weak antiferromagnetic interaction which arises mainly due to super-exchange interaction. The θ_{CW} value in a three-dimensional hyperkagome lattice $\text{Li}_3\text{Yb}_3\text{Te}_2\text{O}_{12}$ with a similar oxygen environment is almost the same order of magnitude at high temperature as well as at low temperature as compared to the present hyperkagome material [39]. ESR spectra taken on polycrystalline samples of $\text{Yb}_3\text{Sc}_2\text{Ga}_3\text{O}_{12}$ are found to be relatively broad with a highly asymmetric shape which is related to magnetic anisotropy and most likely also the distribution of Yb^{3+} moments [61]. The specific heat experiment which is very sensitive to probe magnetic phase transition rules out a long-range magnetic order down to 130 mK in this frustrated magnet. The broad maximum around 200 mK in specific heat data taken in zero field is ascribed to the development of short-range spin correlations at low temperature. The development of short-range spin correlations suggesting the dominance of quantum effects at low temperature that lead to a dynamic liquid-like state in this 3D frustrated antiferromagnet. Similar broad maximum in specific heat at low temperature was also observed in its sister compound $\text{Yb}_3\text{Ga}_5\text{O}_{12}$ [45, 65]. The low temperature magnetic behavior can be described by $J_{\text{eff}} = 1/2$ Kramers doublet ground state as the energy levels of the excited Kramers doublets is well above the ground state, which is confirmed by our CEF calculations. This family of $\text{R}_3\text{Sc}_2\text{Ga}_3\text{O}_{12}$ rare-earth magnetic materials with a suitable choice of rare-earth and non-magnetic cations has a great potential to host non-trivial quantum states with exotic excitations.

IV. CONCLUSION

In summary, we have successfully synthesized and characterized a three-dimensional hyperkagome garnet, namely $\text{Yb}_3\text{Sc}_2\text{Ga}_3\text{O}_{12}$. Magnetization data indicate the absence of long-range magnetic ordering and spin freezing down to 1.8 K. Specific heat measurements reveal that there is no long-range magnetic ordering down to 130 mK. A weak antiferromagnetic exchange interaction is present in this system, which is typical for rare-earth-based magnetic materials due to the localized $4f$ moments. In addition, the absence of ZFC-FC splitting rules out the formation of a glassy phase in this antiferromagnet. Our thermodynamic results indicate that the Yb^{3+} ions are in the Kramers doublet state with an effective $J_{\text{eff}} = 1/2$ spin degrees of freedom at low temperature. Furthermore, ESR results indicate the existence of magnetic anisotropy. The presence of a broad maximum around 200 mK in the temperature dependence of specific heat suggests that a short-range spin correlation phenomena at play in this frustrated magnet. Our CEF modeling suggests that the ground state is well separated from the excited states and yields a very good agreement with thermodynamic and ESR results. Given the fact that the exchange interaction is weak in $4f$ systems, further low-temperature thermodynamic and muon spin relaxation experiments are required to track the ground state properties unambiguously. Microscopic experiments such as neutron scattering are desired to shed insights into the spin-orbit driven anisotropy driving novel ground state arises from the crystal-field splitting of the rare-earth multiplet. Understanding the spin anisotropy and low energy spin excitation spectra sets an interesting track to reveal interesting insights into the ground state properties of this novel frustrated magnet. This family of rare-earth hyperkagome $\text{R}_3\text{Sc}_2\text{Ga}_3\text{O}_{12}$ ($\text{R} = \text{rare-earth}$) offers a promising platform for the experimental realization of unconventional ground states borne out of spin correlation, frustration and spin-orbit driven anisotropy.

V. ACKNOWLEDGMENT

PK acknowledges the funding by the Science and Engineering Research Board, and Department of Science and Technology, India through Research Grants. MP acknowledges the funding by the Slovenian Research Agency (project J2-2513, and program No. P1-0125).

-
- [1] H. T. Diep, *Frustrated Spin Systems* (WORLD SCIENTIFIC, 2005).
 - [2] C. Lacroix, P. Mendels, and F. Mila, eds., *Introduction to Frustrated Magnetism: Materials, Experiments, Theory (Springer Series in Solid-State Sciences)*, 2011th ed. (Springer, 2011).
 - [3] L. Savary and L. Balents, Quantum spin liquids: a review, *Reports on Progress in Physics* **80**, 016502 (2016).
 - [4] Y. Zhou, K. Kanoda, and T.-K. Ng, Quantum spin liquid states, *Rev. Mod. Phys.* **89**, 025003 (2017).
 - [5] P. Anderson, Resonating valence bonds: A new kind of insulator?, *Materials Research Bulletin* **8**, 153 (1973).
 - [6] L. Balents, Spin liquids in frustrated magnets, *Nature* **464**, 199 (2010).
 - [7] S.-H. Do, S.-Y. Park, J. Yoshitake, J. Nasu, Y. Motome, Y. Kwon, D. T. Adroja, D. J. Voneshen, K. Kim, T.-H. Jang,

- J.-H. Park, K.-Y. Choi, and S. Ji, Majorana fermions in the Kitaev quantum spin system α -RuCl₃, *Nature Physics* **13**, 1079 (2017).
- [8] A. Banerjee, C. A. Bridges, J.-Q. Yan, A. A. Aczel, L. Li, M. B. Stone, G. E. Granroth, M. D. Lumsden, Y. Yiu, J. Knolle, S. Bhattacharjee, D. L. Kovrizhin, R. Moessner, D. A. Tennant, D. G. Mandrus, and S. E. Nagler, Proximate kitaev quantum spin liquid behaviour in a honeycomb magnet, *Nature Materials* **15**, 733 (2016).
- [9] C. Broholm, R. J. Cava, S. A. Kivelson, D. G. Nocera, M. R. Norman, and T. Senthil, Quantum spin liquids, *Science* **367**, eaay0668 (2020).
- [10] Y. Shimizu, K. Miyagawa, K. Kanoda, M. Maesato, and G. Saito, Spin liquid state in an organic mott insulator with a triangular lattice, *Phys. Rev. Lett.* **91**, 107001 (2003).
- [11] T. Itou, A. Oyamada, S. Maegawa, M. Tamura, and R. Kato, Quantum spin liquid in the spin-1/2 triangular antiferromagnet EtMe₃Sb[Pd(dmit)₂]₂, *Phys. Rev. B* **77**, 104413 (2008).
- [12] H. D. Zhou, E. S. Choi, G. Li, L. Balicas, C. R. Wiebe, Y. Qiu, J. R. D. Copley, and J. S. Gardner, Spin Liquid State in the $S = 1/2$ Triangular Lattice Ba₃CuSb₂O₉, *Phys. Rev. Lett.* **106**, 147204 (2011).
- [13] P. Khuntia, R. Kumar, A. V. Mahajan, M. Baenitz, and Y. Furukawa, Spin liquid state in the disordered triangular lattice Sc₂Ga₂CuO₇ revealed by NMR, *Phys. Rev. B* **93**, 140408 (2016).
- [14] M. P. Shores, E. A. Nytko, B. M. Bartlett, and D. G. Nocera, A Structurally Perfect $S = 1/2$ Kagome Antiferromagnet, *Journal of the American Chemical Society* **127**, 13462 (2005).
- [15] A. Olariu, P. Mendels, F. Bert, F. Duc, J. C. Trombe, M. A. de Vries, and A. Harrison, ¹⁷O NMR Study of the Intrinsic Magnetic Susceptibility and Spin Dynamics of the Quantum Kagome Antiferromagnet ZnCu₃(OH)₆Cl₂, *Phys. Rev. Lett.* **100**, 087202 (2008).
- [16] P. Khuntia, M. Velazquez, Q. Barthélemy, F. Bert, E. Kermarrec, A. Legros, B. Bernu, L. Messio, A. Zorko, and P. Mendels, Gapless ground state in the archetypal quantum kagome antiferromagnet ZnCu₃(OH)₆Cl₂, *Nature Physics* **16**, 469 (2020).
- [17] Y. Li, H. Liao, Z. Zhang, S. Li, F. Jin, L. Ling, L. Zhang, Y. Zou, L. Pi, Z. Yang, J. Wang, Z. Wu, and Q. Zhang, Gapless quantum spin liquid ground state in the two-dimensional spin-1/2 triangular antiferromagnet YbMgGaO₄, *Scientific Reports* **5**, 16419 (2015), article.
- [18] Y. Li, D. Adroja, R. I. Bewley, D. Vonshen, A. A. Tsirlin, P. Gegenwart, and Q. Zhang, Crystalline Electric-Field Randomness in the Triangular Lattice Spin-Liquid YbMgGaO₄, *Phys. Rev. Lett.* **118**, 107202 (2017).
- [19] Y. Li, S. Bachus, B. Liu, I. Radelytskiy, A. Bertin, A. Schneidewind, Y. Tokiwa, A. A. Tsirlin, and P. Gegenwart, Rearrangement of Uncorrelated Valence Bonds Evidenced by Low-Energy Spin Excitations in YbMgGaO₄, *Phys. Rev. Lett.* **122**, 137201 (2019).
- [20] I. Kimchi, A. Nahum, and T. Senthil, Valence Bonds in Random Quantum Magnets: Theory and Application to YbMgGaO₄, *Phys. Rev. X* **8**, 031028 (2018).
- [21] H. Takagi, T. Takayama, G. Jackeli, G. Khaliullin, and S. E. Nagler, Concept and realization of kitaev quantum spin liquids, *Nature Reviews Physics* **1**, 264 (2019).
- [22] L. Clark, G. Sala, D. D. Maharaj, M. B. Stone, K. S. Knight, M. T. F. Telling, X. Wang, X. Xu, J. Kim, Y. Li, S.-W. Cheong, and B. D. Gaulin, Two-dimensional spin liquid behaviour in the triangular-honeycomb antiferromagnet TbInO₃, *Nature Physics* **15**, 262 (2019).
- [23] T. Arh, B. Sana, M. Pregelj, P. Khuntia, Z. Jagličić, M. D. Le, P. K. Biswas, P. Manuel, L. Mangin-Thro, A. Ozarowski, and A. Zorko, The ising triangular-lattice antiferromagnet neodymium heptatantalate as a quantum spin liquid candidate, *Nature Materials* **21**, 416 (2022).
- [24] B. Koteswararao, R. Kumar, P. Khuntia, S. Bhowal, S. K. Panda, M. R. Rahman, A. V. Mahajan, I. Dasgupta, M. Baenitz, K. H. Kim, and F. C. Chou, Magnetic properties and heat capacity of the three-dimensional frustrated $S = 1/2$ antiferromagnet PbCuTe₂O₆, *Phys. Rev. B* **90**, 035141 (2014).
- [25] P. Khuntia, F. Bert, P. Mendels, B. Koteswararao, A. V. Mahajan, M. Baenitz, F. C. Chou, C. Baines, A. Amato, and Y. Furukawa, Spin Liquid State in the 3D Frustrated Antiferromagnet PbCuTe₂O₆: NMR and Muon Spin Relaxation Studies, *Phys. Rev. Lett.* **116**, 107203 (2016).
- [26] S. Chillal, Y. Iqbal, H. O. Jeschke, J. A. Rodriguez-Rivera, R. Bewley, P. Manuel, D. Khalyavin, P. Steffens, R. Thomale, A. T. M. N. Islam, J. Reuther, and B. Lake, Evidence for a three-dimensional quantum spin liquid in PbCuTe₂O₆, *Nature Communications* **11**, 2348 (2020).
- [27] C. Balz, B. Lake, J. Reuther, H. Luetkens, R. Schönemann, T. Herrmannsdörfer, Y. Singh, A. T. M. Nazmul Islam, E. M. Wheeler, J. Rodriguez-Rivera, T. Guidi, G. Simeoni, C. Baines, and H. Ryll, Physical realization of a quantum spin liquid based on a complex frustration mechanism, *Nature Physics* **12**, 942 (2016).
- [28] C. Balz, B. Lake, A. T. M. Nazmul Islam, Y. Singh, J. A. Rodriguez-Rivera, T. Guidi, E. M. Wheeler, G. G. Simeoni, and H. Ryll, Magnetic Hamiltonian and phase diagram of the quantum spin liquid Ca₁₀Cr₇O₂₈, *Phys. Rev. B* **95**, 174414 (2017).
- [29] K. W. Plumb, H. J. Changlani, A. Scheie, S. Zhang, J. W. Krizan, J. A. Rodriguez-Rivera, Y. Qiu, B. Winn, R. J. Cava, and C. L. Broholm, Continuum of quantum fluctuations in a three-dimensional $S = 1$ Heisenberg magnet, *Nature Physics* **15**, 54 (2019).
- [30] B. Gao, T. Chen, D. W. Tam, C.-L. Huang, K. Sasmal, D. T. Adroja, F. Ye, H. Cao, G. Sala, M. B. Stone, C. Baines, J. A. T. Verezhak, H. Hu, J.-H. Chung, X. Xu, S.-W. Cheong, M. Nallaiyan, S. Spagna, M. B. Maple, A. H. Nevidomskyy, E. Morosan, G. Chen, and P. Dai, Experimental signatures of a three-dimensional quantum spin liquid in effective spin-1/2 Ce₂Zr₂O₇ pyrochlore, *Nature Physics* **15**, 1052 (2019).
- [31] J. Gaudet, E. M. Smith, J. Dudemaine, J. Beare, C. R. C. Buhariwalla, N. P. Butch, M. B. Stone, A. I. Kolesnikov, G. Xu, D. R. Yahne, K. A. Ross, C. A. Marjerrison, J. D. Garrett, G. M. Luke, A. D. Bianchi, and B. D. Gaulin, Quantum Spin Ice Dynamics in the Dipole-Octupole Pyrochlore Magnet Ce₂Zr₂O₇, *Phys. Rev. Lett.* **122**, 187201 (2019).
- [32] Y.-D. Li and G. Chen, Symmetry enriched u(1) topological orders for dipole-octupole doublets on a pyrochlore lattice, *Phys. Rev. B* **95**, 041106 (2017).
- [33] E. M. Smith, O. Benton, D. R. Yahne, B. Placke, R. Schäfer, J. Gaudet, J. Dudemaine, A. Fitterman, J. Beare, A. R. Wildes, S. Bhattacharya, T. DeLazzer, C. R. C. Buhariwalla, N. P. Butch, R. Movshovich, J. D. Garrett, C. A. Marjerrison, J. P. Clancy, E. Kermarrec, G. M. Luke, A. D. Bianchi, K. A. Ross, and B. D. Gaulin, Case for a U(1)_π Quantum Spin Liquid Ground State in the Dipole-Octupole Pyrochlore Ce₂Zr₂O₇, *Phys. Rev. X* **12**, 021015 (2022).
- [34] Y. Okamoto, M. Nohara, H. Aruga-Katori, and H. Takagi, Spin-Liquid State in the $S = 1/2$ Hyperkagome Antiferromagnet Na₄Ir₃O₈, *Phys. Rev. Lett.* **99**, 137207 (2007).

- [35] Y. Zhou, P. A. Lee, T.-K. Ng, and F.-C. Zhang, $\text{Na}_4\text{Ir}_3\text{O}_8$ as a 3D Spin Liquid with Fermionic Spinons, *Phys. Rev. Lett.* **101**, 197201 (2008).
- [36] M. J. Lawler, H.-Y. Kee, Y. B. Kim, and A. Vishwanath, Topological Spin Liquid on the Hyperkagome Lattice of $\text{Na}_4\text{Ir}_3\text{O}_8$, *Phys. Rev. Lett.* **100**, 227201 (2008).
- [37] A. C. Shockley, F. Bert, J.-C. Orain, Y. Okamoto, and P. Mendels, Frozen State and Spin Liquid Physics in $\text{Na}_4\text{Ir}_3\text{O}_8$: An NMR Study, *Phys. Rev. Lett.* **115**, 047201 (2015).
- [38] D. I. Khomskii, *Transition Metal Compounds* (Cambridge University Press, 2014).
- [39] J. Khatua, S. Bhattacharya, Q. P. Ding, S. Vrtnik, A. M. Strydom, N. P. Butch, H. Luetkens, E. Kermarrec, M. S. R. Rao, A. Zorko, Y. Furukawa, and P. Khuntia, Spin liquid state in a rare-earth hyperkagome lattice, *Phys. Rev. B* **106**, 104404 (2022).
- [40] P. Mukherjee, A. C. S. Hamilton, H. F. J. Glass, and S. E. Dutton, Sensitivity of magnetic properties to chemical pressure in lanthanide garnets $\text{Ln}_3\text{A}_2\text{X}_3\text{O}_{12}$, $\text{Ln} = \text{Gd, Tb, Dy, Ho, A} = \text{Ga, Sc, In, Te, X} = \text{Ga, Al, Li}$, *Journal of Physics: Condensed Matter* **29**, 405808 (2017).
- [41] J. A. M. Paddison, H. Jacobsen, O. A. Petrenko, M. T. Fernández-Díaz, P. P. Deen, and A. L. Goodwin, Hidden order in spin-liquid $\text{Gd}_3\text{Ga}_5\text{O}_{12}$, *Science* **350**, 179 (2015).
- [42] H. Jacobsen, O. Florea, E. Lhotel, K. Lefmann, O. A. Petrenko, C. S. Knee, T. Seydel, P. F. Henry, R. Bewley, D. Vonshen, A. Wildes, G. Nilsen, and P. P. Deen, Spin dynamics of the director state in frustrated hyperkagome systems, *Phys. Rev. B* **104**, 054440 (2021).
- [43] Y. Machida, S. Nakatsuji, S. Onoda, T. Tayama, and T. Sakakibara, Time-reversal symmetry breaking and spontaneous hall effect without magnetic dipole order, *Nature* **463**, 210 (2010).
- [44] L. O. Sandberg, R. Edberg, I.-M. B. Bakke, K. S. Pedersen, M. C. Hatnean, G. Balakrishnan, L. Mangin-Thro, A. Wildes, B. Fåk, G. Ehlers, G. Sala, P. Henelius, K. Lefmann, and P. P. Deen, Emergent magnetic behavior in the frustrated $\text{Yb}_3\text{Ga}_5\text{O}_{12}$ garnet, *Phys. Rev. B* **104**, 064425 (2021).
- [45] P. Dalmas de Réotier, A. Yaouanc, P. C. M. Gubbens, C. T. Kaiser, C. Baines, and P. J. C. King, Absence of Magnetic Order in $\text{Yb}_3\text{Ga}_5\text{O}_{12}$: Relation between Phase Transition and Entropy in Geometrically Frustrated Materials, *Phys. Rev. Lett.* **91**, 167201 (2003).
- [46] J. A. Hodges, P. Bonville, M. Rams, and K. K. Ias, *Journal of Physics: Condensed Matter* **15**, 4631 (2003).
- [47] Y. Cai, M. N. Wilson, J. Beare, C. Lygouras, G. Thomas, D. R. Yahne, K. Ross, K. M. Taddei, G. Sala, H. A. Dabkowska, A. A. Aczel, and G. M. Luke, Crystal fields and magnetic structure of the Ising antiferromagnet $\text{Er}_3\text{Ga}_5\text{O}_{12}$, *Phys. Rev. B* **100**, 184415 (2019).
- [48] N. Zhao, H. Ge, L. Zhou, Z. M. Song, J. Yang, T. T. Li, L. Wang, Y. Fu, Y. F. Zhang, J. B. Xu, S. M. Wang, J. W. Mei, X. Tong, L. S. Wu, and J. M. Sheng, Antiferromagnetism and Ising ground states in the rare-earth garnet $\text{Nd}_3\text{Ga}_5\text{O}_{12}$, *Phys. Rev. B* **105**, 014441 (2022).
- [49] N. F. Chilton, R. P. Anderson, L. D. Turner, A. Soncini, and K. S. Murray, PHI: A powerful new program for the analysis of anisotropic monomeric and exchange-coupled polynuclear d- and f-block complexes, *J. Comput. Chem.* **34**, 1164 (2013).
- [50] J. Rodríguez-Carvajal, Recent advances in magnetic structure determination by neutron powder diffraction, *Physica B: Condensed Matter* **192**, 55 (1993).
- [51] K. Momma and F. Izumi, *VESTA3* for three-dimensional visualization of crystal, volumetric and morphology data, *Journal of Applied Crystallography* **44**, 1272 (2011).
- [52] R. A. Buchanan, K. A. Wickersheim, J. J. Pearson, and G. F. Herrmann, Energy Levels of Yb^{3+} in Gallium and Aluminum Garnets. I. Spectra, *Phys. Rev.* **159**, 245 (1967).
- [53] V. Simonet, R. Ballou, J. Robert, B. Canals, F. Hippert, P. Bordet, P. Lejay, P. Fouquet, J. Ollivier, and D. Braithwaite, Hidden Magnetic Frustration by Quantum Relaxation in Anisotropic Nd Langasite, *Phys. Rev. Lett.* **100**, 237204 (2008).
- [54] Y. Shen, Y.-D. Li, H. Wo, Y. Li, S. Shen, B. Pan, Q. Wang, H. C. Walker, P. Steffens, M. Boehm, Y. Hao, D. L. Quintero-Castro, L. W. Harriger, M. D. Frontzek, L. Hao, S. Meng, Q. Zhang, G. Chen, and J. Zhao, Evidence for a spinon fermi surface in a triangular-lattice quantum-spin-liquid candidate, *Nature* **540**, 559 (2016).
- [55] E. Lhotel, L. Mangin-Thro, E. Ressouche, P. Steffens, E. Bichaud, G. Knebel, J.-P. Brison, C. Marin, S. Raymond, and M. E. Zhitomirsky, Spin dynamics of the quantum dipolar magnet $\text{Yb}_3\text{Ga}_5\text{O}_{12}$ in an external field, *Phys. Rev. B* **104**, 024427 (2021).
- [56] J. Jensen and A. R. Mackintosh, *Rare Earth Magnetism: Structures and Excitations* (Oxford Science Publications. Clarendon Press, 1991).
- [57] S. S. Sosin, A. F. Iafarova, I. V. Romanova, O. A. Morozov, S. L. Korableva, R. G. Batulin, M. Zhitomirsky, and V. N. Glazkov, Microscopic Spin Hamiltonian for a Dipolar Heisenberg Magnet LiGdF_4 from EPR Measurements, *JETP Letters* **116**, 771 (2022).
- [58] A. C. S. Hamilton, G. I. L. and S E Rowley, and S. E. Dutton, Enhancement of the magnetocaloric effect driven by changes in the crystal structure of Al-doped GGG, $\text{Gd}_3\text{Ga}_{5-x}\text{Al}_x\text{O}_{12}$ ($0 \leq x \leq 5$), *Journal of Physics: Condensed Matter* **26**, 116001 (2014).
- [59] Z.-X. Luo, E. Lake, J.-W. Mei, and O. A. Starykh, Spinon magnetic resonance of quantum spin liquids, *Phys. Rev. Lett.* **120**, 037204 (2018).
- [60] K. Somesh, S. S. Islam, S. Mohanty, G. Simutis, Z. Guguchia, C. Wang, J. Sichelschmidt, M. Baenitz, and R. Nath, Absence of magnetic order and emergence of unconventional fluctuations in the $J_{\text{eff}} = \frac{1}{2}$ triangular-lattice antiferromagnet YbBO_3 , *Phys. Rev. B* **107**, 064421 (2023).
- [61] H. Benner, M. Brodehl, H. Seitz, and J. Wiese, Influence of nondiagonal dynamic susceptibility on the epr signal of heisenberg magnets, *Journal of Physics C: Solid State Physics* **16**, 6011 (1983).
- [62] A. Tari, *The specific heat of matter at low temperatures* (World Scientific, 2003).
- [63] E. Gopal, *Specific heats at low temperatures* (Springer Science & Business Media, 2012).
- [64] C. Y. Jiang, Y. X. Yang, Y. X. Gao, Z. T. Wan, Z. H. Zhu, T. Shiroka, C. S. Chen, Q. Wu, X. Li, J. C. Jiao, K. W. Chen, Y. Bao, Z. M. Tian, and L. Shu, Spin excitations in the quantum dipolar magnet $\text{Yb}(\text{BaBO}_3)_3$, *Phys. Rev. B* **106**, 014409 (2022).
- [65] J. Filippi, J. C. Lasjaunias, B. Hebral, J. Rossat-Mignod, and F. Tcheou, Magnetic properties of ytterbium gallium garnet between 44 mK and 4 K, *Journal of Physics C: Solid State Physics* **13**, 1277 (1980).
- [66] O. V. Lounasmaa, Specific Heat of Holmium Metal between 0.38 and 4.2°K, *Phys. Rev.* **128**, 1136 (1962).
- [67] Y. Takeda, N. Duc Dung, Y. Nakano, T. Ishikura, S. Ikeda, T. D. Matsuda, E. Yamamoto, Y. Haga, T. Takeuchi, R. Settai, and Y. Ōnuki, Calorimetric Study in Single Crystalline RCu_2Si_2 (R: Rare Earth), *Journal of the Physical Society of Japan* **77**, 104710 (2008).

- [68] S. Kundu, A. Shahee, A. Chakraborty, K. M. Ranjith, B. Koo, J. Sichelschmidt, M. T. F. Telling, P. K. Biswas, M. Baenitz, I. Dasgupta, S. Pujari, and A. V. Mahajan, Gapless Quantum Spin Liquid in the Triangular System $\text{Sr}_3\text{CuSb}_2\text{O}_9$, *Phys. Rev. Lett.* **125**, 267202 (2020).
- [69] T. Dey, A. V. Mahajan, P. Khuntia, M. Baenitz, B. Koteswararao, and F. C. Chou, Spin-liquid behavior in $J_{\text{eff}} = \frac{1}{2}$ triangular lattice compound $\text{Ba}_3\text{IrTi}_2\text{O}_9$, *Phys. Rev. B* **86**, 140405 (2012).
- [70] M. A. de Vries, K. V. Kamenev, W. A. Kockelmann, J. Sanchez-Benitez, and A. Harrison, Magnetic Ground State of an Experimental $S = 1/2$ Kagome Antiferromagnet, *Phys. Rev. Lett.* **100**, 157205 (2008).
- [71] J. A. M. Paddison, M. Daum, Z. Dun, G. Ehlers, Y. Liu, M. Stone, H. Zhou, and M. Mourigal, Continuous excitations of the triangular-lattice quantum spin liquid YbMgGaO_4 , *Nature Physics* **13**, 117 (2017).
- [72] M. Baenitz, P. Schlender, J. Sichelschmidt, Y. A. Onyikienko, Z. Zangeneh, K. M. Ranjith, R. Sarkar, L. Hozoi, H. C. Walker, J.-C. Orain, H. Yasuoka, J. van den Brink, H. H. Klauss, D. S. Inosov, and T. Doert, NaYbS_2 : A planar spin- $\frac{1}{2}$ triangular-lattice magnet and putative spin liquid, *Phys. Rev. B* **98**, 220409 (2018).
- [73] S. Yamashita, Y. Nakazawa, M. Oguni, Y. Oshima, H. Nojiri, Y. Shimizu, K. Miyagawa, and K. Kanoda, Thermodynamic properties of a spin-1/2 spin-liquid state in a κ -type organic salt, *Nature Physics* **4**, 459 (2008).
- [74] S. Yamashita, T. Yamamoto, Y. Nakazawa, M. Tamura, and R. Kato, Gapless spin liquid of an organic triangular compound evidenced by thermodynamic measurements, *Nature Communications* **2**, 275 (2011).
- [75] K. W. H. Stevens, Matrix elements and operator equivalents connected with the magnetic properties of rare earth ions, *Proc. Phys. Soc.* **65**, 209 (1952).
- [76] L. Ø. Sandberg, R. Edberg, I.-M. B. Bakke, K. S. Pedersen, M. C. Hatnean, G. Balakrishnan, L. Mangin-Thro, A. Wildes, B. Fåk, G. Ehlers, *et al.*, Emergent magnetic behavior in the frustrated $\text{Yb}_3\text{Ga}_5\text{O}_{12}$ garnet, *Phys. Rev. B* **104**, 064425 (2021).